frontiers | Frontiers in Marine Science

TYPE Original Research
PUBLISHED 28 January 2025
DOI 10.3389/fmars.2025.1461723

OPEN ACCESS

EDITED BY
Alex J. Poulton,
Heriot-Watt University, United States

REVIEWED BY
Kathryn Barbara Cook,
University of Exeter, United Kingdom
Réka Domokos,
National Oceanic and Atmospheric Administration (NOAA), United States
Ping Du,
Ministry of Natural Resources, China

*CORRESPONDENCE
Katherine Baker
katherine.baker@utas.edu.au

RECEIVED 09 July 2024
ACCEPTED 03 January 2025
PUBLISHED 28 January 2025

CITATION
Baker K, Halfter S, Scoulding B, Swadling KM, Richards SA, Bressac M, Sutton CA and Boyd PW (2025) Carbon injection potential of the mesopelagic-migrant pump in the Southern Ocean during summer.
Front. Mar. Sci. 12:1461723.
doi: 10.3389/fmars.2025.1461723

Carbon injection potential of the mesopelagic-migrant pump in the Southern Ocean during summer

Katherine Baker[1,2]*, Svenja Halfter[1,3], Ben Scoulding[4], Kerrie M. Swadling[1,2], Shane A. Richards[5], Matthieu Bressac[1,6], Caroline A. Sutton[4] and Philip W. Boyd[1,2]

[1]Institute for Marine and Antarctic Studies, University of Tasmania, Hobart, TAS, Australia, [2]Australian Antarctic Program Partnership, University of Tasmania, Hobart, TAS, Australia, [3]National Institute of Water and Atmospheric Research, Wellington, New Zealand, [4]Environment, Commonwealth Scientific and Industrial Research Organisation (CSIRO), Hobart, TAS, Australia, [5]School of Natural Sciences, University of Tasmania, Hobart, TAS, Australia, [6]Sorbonne Université, CNRS, Laboratoire d'Océanographie de Villefranche, LOV, Villefranche-sur-Mer, France

The passive sinking flux of particles, termed the biological gravitational pump (BGP), is an important component of the ocean's biological carbon pump. In addition, carbon-rich particles are actively injected to depth through the diel vertical migration (DVM) of micronekton and mesozooplankton from the surface to the oceans' twilight zone (200 m – 1000 m depth). This is known as the mesopelagic-migrant pump (MMP). We investigated the magnitude of the MMP at one subantarctic and two polar sites in summer by assessing particulate and dissolved carbon export below 200 m depth based on DVM and the composition of the mesopelagic community. Carbon injection potential (CIP) for the dominant taxa at each site was estimated through four pathways, i.e., excretion, respiration, fecal pellets, and carcass production. Blooms of two migratory tunicate species, the pyrosome *Pyrosoma atlanticum* (subantarctic) and the salp *Salpa thompsoni* (polar) dominated the micronekton biomass and MMP export ranged from 5.0 to 9.4 mg C m^{-2} d^{-1} across the three Southern Ocean sites. Mesozooplankton abundance was dominated by copepods, which contributed an additional 0.7 to 32.2 mg C m^{-2} d^{-1} to the MMP. Results from this summertime study suggest an increase in the relative importance of the MMP compared to the BGP south of the Polar Front, however, future work should target the seasonality of the MMP, which necessitates linking environmental drivers to micronekton and mesozooplankton community composition, life history, and DVM.

KEYWORDS

micronekton, mesozooplankton, Southern Ocean, diel vertical migration, active carbon export

1 Introduction

The biological carbon pump (BCP) is a key process through which carbon dioxide fixed by primary producers is transported from the sea surface to the deep layers of the ocean (Buesseler and Boyd, 2009). Carbon is considered exported once it is transported below the permanent pycnocline as it is no longer in communication with the atmosphere on timescales of years (Boyd and Trull, 2007). When this exported carbon is remineralized into dissolved inorganic carbon (DIC) it is no longer biologically available for consumers and, depending on the depth of remineralization (Kwon et al., 2009), has the potential to be sequestered in the deep ocean for centuries (Boyd et al., 2019; Nowicki et al., 2022; Nowicki et al., 2024; Frenger et al., 2024). Recent studies suggest that our conventional understanding of the underlying mechanisms driving this process, namely through the passive sinking of carbon-rich particles, termed the biological gravitational pump (BGP), is too simplistic (Boyd et al., 2019; Dall'Olmo et al., 2016; Jónasdóttir et al., 2015; Omand et al., 2015). Boyd et al. (2019) review a range of processes, collectively referred to as particle injection pumps (PIPs), through which particles can be transported to depth. These mechanisms include the physically mediated eddy-subduction pump, the mixed-layer pump, the biologically driven seasonal lipid pump (e.g., copepod diapause at depth), and the mesopelagic-migrant pump. Therefore, downward export driven by the biological carbon pump is a combination of both passive and active transport processes.

One understudied mode of particle injection is the mesopelagic-migrant pump (MMP), which is the active movement of carbon by micronekton and mesozooplankton between the epipelagic zone (0 - 200 m) and the mesopelagic/twilight zone (200 m – 1000 m) (Boyd et al., 2019). This daily movement of biota is referred to as DVM (diel vertical migration) (Bandara et al., 2021). Through the MMP, a proportion of carbon-rich living and non-living particles ingested in the upper 200 m at night is actively transported below the epipelagic zone to an individual's preferred habitat depth in the twilight zone during the day (Annasawmy et al., 2019; John et al., 2016). While a substantial portion of the carbon ingested at the surface is retained as living carbon, represented by the community's biomass, the MMP specifically reflects the non-living component.

Both mesozooplankton (0.2-20 mm length) and micronekton (20-200 mm length) are taxonomically diverse pelagic groups that connect primary and secondary production to higher trophic level consumers such as fish, marine mammals, and seabirds (Steinberg and Landry, 2017). They include copepods, pelagic tunicates (larvaceans, salps, pyrosomes), mesopelagic fish, krill, and other crustaceans (e.g. prawns, amphipods), chaetognaths and jellyfish (Kwong et al., 2020). While DVM is well documented from deep scattering layers imaged through ship acoustics (e.g. Bandara et al., 2021), the magnitude of the contribution that migrating micronekton and, to a lesser extent mesozooplankton, make to biogeochemical cycling in the ocean is still under debate (Kelly et al., 2019). Micronekton and mesozooplankton release carbon via four main pathways: excretion, in the form of dissolved organic carbon (DOC) (Steinberg et al., 2000); respiration, as dissolved inorganic carbon (DIC) (Ariza et al., 2015; Davison et al., 2013); fecal pellets, as particulate organic carbon (POC) (Phillips et al., 2009; Saba et al., 2021); and carcasses, as POC (Halfter et al., 2021).

When individuals release carbon in the mesopelagic zone after feeding at the sea surface it is considered active carbon export (Kwong et al., 2020; Steinberg and Landry, 2017). This active carbon export is seldom accounted for when estimating downward export through the biological carbon pump by traditional sampling methods (e.g., sediment traps (Steinberg and Landry, 2017)). Unlike the passive sinking of particles across the mixed layer, active carbon export by animals undertaking DVM allows particles to escape microbial remineralization in surface waters, shunting carbon to the deep sea (Aumont et al., 2018; Boyd et al., 2019). However, not all taxa contribute to the MMP equally. Their contribution is contingent on the carbon injection potential (CIP) of taxa, i.e., the taxon-specific physiological rates that control how much carbon an individual can release in a given time period, and their migratory behavior which controls the fraction of CIP exported to depth from the epipelagic layer (0-200 m depth) (Kwong et al., 2020).

Estimates of the MMP contribution to downward carbon export range from 1.5 to 89% relative to the magnitude of the BGP at the base of the epipelagic zone (Pakhomov et al., 2019; Hernandez-Leon et al., 2019). Uncertainties in the estimated magnitude of the MMP can be attributed to differences in: biomass estimates due to the diverse sampling techniques used (Irigoien et al., 2014; Kwong et al., 2022; Underwood et al., 2020), the taxa studied (e.g. fish-mediated carbon flux (Davison et al., 2013; McMonagle et al., 2023; Saba et al., 2021)), and the techniques used to quantify carbon (e.g., electron transport system (ETS) assays versus respirometry experiments) (Ariza et al., 2015; Belcher et al., 2019). Additional uncertainties are driven by the patchy nature of the horizontal and vertical distribution of different taxonomic groups (Kwong et al., 2020), and the influences of regional oceanography and seasonality on the abundance and community composition of micronekton and mesozooplankton (Cotté et al., 2022; Goldblatt et al., 1999). These uncertainties are in part due to a limited number of observations, owing to difficulties associated with collecting mesopelagic samples in remote locations.

The Southern Ocean represents an important knowledge gap in the quantification of downward carbon export through the biological carbon pump (Nowicki et al., 2022). Despite storing much of the world's oceanic DIC (including natural and anthropogenic CO_2), there is a lack of empirical observations in the Southern Ocean, which presents a challenge for the parameterization of carbon export models (Nowicki et al., 2022). Estimates of high biomass of organisms in the mesopelagic and bathypelagic (> 1000 m depth) zones in some regions of the Southern Ocean suggest that carbon demand at depth exceeds passive carbon export through the BGP alone, signaling an unbalanced carbon budget (Burd et al., 2010; Hernandez-Leon et al., 2020). At regional scales, modeled differences in expected versus observed particle attenuation at depth suggest carbon export may be controlled by processes additional to gravitational sinking and microbial remineralization (Bisson et al., 2018; Boyd et al., 2019; Buesseler and Boyd, 2009). Therefore, interest in

incorporating the MMP into Southern Ocean biogeochemical models has increased both at regional (i.e., reconciling regional carbon budgets) and global scales (i.e., more robust predictions of magnitude and direction of change in the BCP with climate change) (Archibald et al., 2019; Aumont et al., 2018; Nowicki et al., 2022). However, many models do not include trophic levels higher than primary consumers to estimate carbon export (Archibald et al., 2019). Models that include DVM commonly make general assumptions about micronekton and mesozooplankton community composition, physiology, and migration behavior (Anderson et al., 2019).

In this study, we investigated the magnitude of MMP-driven downward carbon export in the Southern Ocean using data collected as part of the Southern Ocean Large Areal Carbon Export (SOLACE) voyage in the summer of December 2020 - January 2021 (Boyd et al., 2024; Thompson et al., 2023). We examined the role of the MMP across three Southern Ocean sites by (1) estimating MMP driven downward carbon export based on micronekton and mesozooplankton community composition and DVM, and (2) determining the importance of the MMP relative to the BGP at 200 m depth. Furthermore, this study presents an empirical dataset for a data-poor region, providing an observational case study that can be used to refine model parameters, namely DVM and biomass, and to improve projections of downward carbon export in the Southern Ocean.

2 Methods

2.1 Study area

Micronekton and mesozooplankton were collected from 5 December 2020 to 15 January 2021 during the SOLACE voyage on the *RV Investigator* at three Southern Ocean sites (Figure 1A). Multi-day sampling was quasi-Lagrangian at all sites and deployments followed a modular 3.5-day cycle. Vertical profiles of temperature (Figure 1B), salinity (Figure 1C), and chlorophyll-a fluorescence (Figure 1D) from the sea surface to 1000 m depth at each site were measured with a Seabird SBE911 CTD 36.

The Southern Ocean Time Series site (SOTS: 47 ° S, 141 ° E) is a high nutrient, low chlorophyll (HNLC) region and is monitored year-round by a suite of pelagic and deeper sensors attached to deep sea moorings (Trull et al., 2010). The SOTS site is situated between the subtropical front to the north and the subantarctic front to the south (Trull et al., 2001) and was chosen as the subantarctic site on SOLACE because it is characterized by a low advective regime, enabling the intercomparison of the MMP and the BGP. Site occupation (December 9 – 20th) occurred during the annual peak in primary productivity, and a subsurface intrusion of warmer, saltier, subtropical water around 125 - 375 m depth was identified (Figures 1B, C).

The two polar sites (P1: 56 ° S, 139 ° E and P2: 58 ° S 141.11 ° E) located south of the Polar Front were characterized by cold, nutrient-rich waters. Each site was selected by using satellite maps of sea surface height anomaly to locate low advection regions (Boyd et al., 2024) similar to those at the SOTS site. Sampling at the polar sites followed a holey sock drogue deployed at mid-depth within the seasonal mixed layer (Boyd et al., 2024). A deep chlorophyll maximum (DCM) was identified at P1 following the methods in Boyd et al. (2024), which indicated that the site occupation (December 24 – 31st) was during a period when primary productivity was declining from the seasonal peak in this region. Further south at P2, site occupation (January 1 – 10th) coincided with peak primary productivity as indicated by the high surface chlorophyll-a (Figure 1D). This north to south progression in chl-a peaks during site occupation was confirmed by ocean color satellite re-analysis from the following months (Boyd et al., 2024).

2.2 Sample collection

Micronekton were sampled using a rectangular midwater trawl net with a 16 m^2 opening (RMT16). The 6.35 mm mesh size and hard cod-end with 750 µm mesh prevented the capture of smaller zooplankton taxa. Oblique tows were conducted through three depth layers: the lower mesopelagic layer (1000-400 m), the upper mesopelagic layer (400-200 m), and the epipelagic layer (200-0 m). Multiple (2-3) tows were conducted during both day and night across consecutive days and nights at each depth layer and site to account for patchiness in the distribution of organisms. The net was equipped with a programmable controller that allowed remote opening/closing of the net mouth for discrete layer sampling and was hauled in at 3 – 5 m min^{-1} at a tow speed of ~1-1.5 knots. Filtered water volume (m^3) was calculated using the tow duration (minutes) multiplied by the average ship speed and net mouth area (average volume: 34,571 m^3). Once on board, specimens were removed from the cod-end, separated into broad taxonomic groups, and then identified to the lowest taxonomic level possible. Lengths of individuals of all groups (to the nearest mm) and wet weights of fish (to the nearest 0.05 g) were measured. If the number of individuals in a group per tow was greater than 30, the lengths of subsamples (n ≥30) were measured. Samples were then frozen at -20° C for further analysis on shore.

In the laboratory micronekton were broadly divided into six taxonomic groups based on morphology as well as physiological rate information available in the literature, namely: crustaceans (e.g. prawns, amphipods), krill, fish, other gelatinous (e.g. siphonophores, medusae), pyrosomes and salps. Cephalopods were excluded from analyses due to their low abundance, which was likely due to net avoidance. Abundance estimates (ind. m^{-3}) were obtained from the number of individuals per tow divided by volume filtered. Biomass (mg C m^{-3}) estimates were obtained by calculating the carbon weight (mg C) of individuals in each higher taxonomic group based on length to weight conversions from the literature (see Supplementary Table 1) and multiplying by the abundance of each group per net tow.

Mesozooplankton were sampled with a 335 µm neuston net (1 m^2 opening) with an attached General Oceanics flowmeter. One day and night oblique tow, with a ship's speed between 0.5-1 knots for 10 min, were conducted from 200-0 m to capture variations in abundance between day and nighttime. Once on board, samples were split using a Motoda box and frozen at -80 ° C for onshore analysis. In the laboratory, samples were split (2 – 6 times

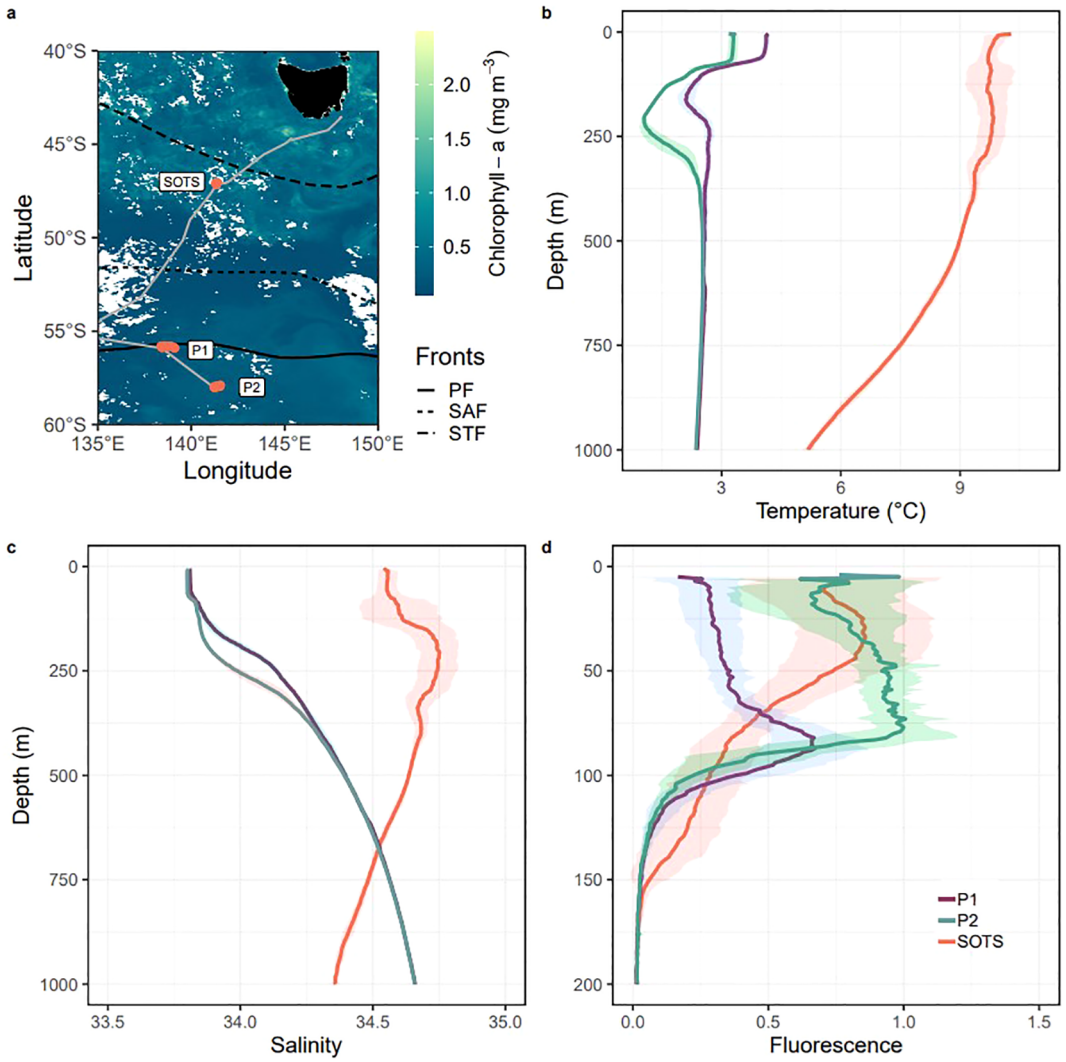

FIGURE 1
(A) Study location in the subantarctic (SOTS) and polar (P1, P2) Southern Ocean south of Tasmania, Australia (shaded in black) including oceanic fronts (PF; Polar Front, SAF; Subantarctic Front; STF; Subtropical Front) overlaid on chl-a concentrations (in mg m^{-3}) in December 2021 derived from satellite data. Cloud cover is indicated by areas in white and sample sites are marked in orange. **(B)** Average CTD derived temperature profiles (° C), **(C)** average salinity (subsurface intrusion of subtropical water identified between 125 - 375 m depth at SOTS) and **(D)** average nighttime chlorophyll fluorescence profiles at SOTS, P1 and P2 to 1000 m depth. Shading represents the range of data across replicate profiles.

depending on sample density) identified and enumerated. Filtered volume calculated from the flowmeter readings and number of splits was used to calculate abundance in ind. m^{-3}.

2.3 Active carbon export

2.3.1 Micronekton

To determine the amount of carbon transported by the migratory micronekton community, we first estimated the carbon injection potential for individuals, denoted CIP (mg C d^{-1}), according to their size (to the nearest mm) and taxonomic group, separately for the day and night tows. Only epipelagic tows (200 – 0 m) were used to determine the migratory proportion of the community. CIP incorporates POC, DIC, and DOC. Using estimates of the carbon potential of individuals, we then upscaled to represent the sampled migratory community. This method allows us to compare values across different taxonomic groups and incorporate size frequency data from each deployment, rather than solely relying on mean sizes of taxa.

Size-dependent CIP components include: respiratory carbon (RC), excretory carbon (EC), carcass carbon (CC), and fecal carbon (FC), which were calculated based on established equations from the literature (Table 1). For FC, we determined the weight of an individual's daily food ball based on their index of stomach fullness (% of total body weight) and assumed an 88% assimilation efficiency (Table 1, Kwong et al., 2020). We also assumed individuals had a full gut upon initiation of downward migration. Whether this ingested material was egested below 200 m depends on how long it takes for food to be assimilated (gut passage time, GPT) and the time it takes for individuals to migrate into the mesopelagic zone (downward migration time; DM). If DM is greater than GPT,

TABLE 1 Components of the carbon injection potential: RO = respiratory oxygen uptake rate (µl O_2 ind^{-1} h^{-1}); RQ = respiratory quotient; 12 = molar weight of carbon (g mol^{-1}); 22.4 = volume of an ideal gas at standard pressure (mol L^{-1}); DW = dry weight (mg); ISF = index of stomach fullness (% of total body weight); FB = food ball weight (mg); E = egestion rate (h); GPT = gut passage time (h); DM = time spent on downward migration (h). These equations incorporate allometric regressions found in the literature (Supplementary Tables 1-3).

CIP Components	Equation	Reference
Respiratory carbon (RC) (mg C ind^{-1} h^{-1})	$RC = RO * RQ * (12/22.4)/1000$	Al-Mutairi and Landry (2001)
Excretory carbon (EC) (mg C ind^{-1} h^{-1})	$EC = RC * 0.00031$	Steinberg et al. (2000)
Carcass carbon (CC) (mg C ind^{-1} h^{-1})	$CC = RC * 0.00066$	Hernandez-Leon et al (2019)
Fecal carbon (FC) (mg C ind^{-1} d^{-1})	$FB = DW * ISF$ $E = 0.12 * FB$ $FC = (E/24) * \max(0, GPT - DM)/1000$	Kwong et al. (2020)

export of pellets does not occur (Table 1). We also assumed migrating individuals did not feed at depth.

CIP (mg C d^{-1}) at depth by an individual over the course of a day was calculated using

$$CIP = (RC + EC + CC) * TD + FC \quad (1)$$

where TD is time spent at depth (h). For nocturnal migration TD is hours of daylight, whereas for reverse migration TD is hours of darkness. The average period of daylight was 15.8 h at SOTS, 17.2 h at P1 and 17.6 h at P2.

The daily export of carbon (CE, mg C m^{-2} d^{-1}) for a tow per taxonomic group t is given by

$$CE_t = p_t A_t \sum_l f_{lt} CIP_{lt} \quad (2)$$

where A_t (ind m^{-2}) is the abundance of the group, p_t is the proportion of these individuals that migrate, f_{lt} is the proportion of individuals in the group that are of length l, and CIP_{lt} is the carbon injection potential for an individual in the group of length l. The migrating proportion was estimated using

$$p_t = \frac{|A_t^{night} - A_t^{day}|}{\max(A_t^{night}, A_t^{day})} \quad (3)$$

where A_t^{night} and A_t^{day} are the abundances associated with night and day epipelagic tows. Total carbon export (mg C m^{-2} d^{-1}) is the sum of taxon specific export per tow;

$$CE = \sum_t CE_t \quad (4)$$

To address uncertainty in total carbon export based on differences in abundances between replicate micronekton tows, combinations of day and night tow abundances were bootstrapped 1000 times (Efron and Tibshirani, 1993; Smith et al., 2023). Carbon export per site was estimated by taking the bootstrapped mean CE (mg C m^{-2} d^{-1}). Bootstrapped mean and standard deviation per site reflect the spread of carbon export estimates from replicate deployments with 95% confidence. Bootstrapping CIPs enabled us to establish an uncertainty range around estimates, reflecting differences in abundance between trawls. However, bootstrapping does not account for potential temporal fluctuations in abundance between deployments caused by varying environmental conditions.

2.3.2 Mesozooplankton

For mesozooplankton active carbon transport calculations, only the copepod community was included due to insufficient length and weight data for the rest of the mesozooplankton community. However, with copepods contributing over 80% of the total abundance per deployment, these estimates are considered representative. For the copepod community, CIP per individual was calculated similarly to micronekton. However, due to the limited data the average sizes of prevalent copepod species across all sites were used.

At SOTS, *Neocalanus tonsus* and *Oithona* spp. were the dominant taxa identified, while *Rhincalanus gigas* and *Oithona* spp. were prevalent at both polar sites. Prosome lengths of at least 100 individuals of *N. tonsus* and *R. gigas* were measured from each deployment. For *Oithona* spp., average length and weight values from the literature were used (Mizdalski, 1988). The average carbon weight of the three taxa was determined by applying length-to-dry-weight (L-to-DW) allometric equations to the average subsampled length measured at each site—or, in the case of *Oithona* spp., the average length from the literature. Carbon weight was assumed to be 0.4 times the dry weight (DW), following Steinberg et al. (2000). The calculated CIP values, based on the average length of each species (and site-specific values for *R. gigas*), were applied to the entire copepod community proportionally to their relative abundance in each deployment. As replicate tows were unavailable, bootstrapping was not performed. Carbon export from the copepod community was estimated as the difference between night and day CIP at each site.

2.4 Gravitational flux measurements

Downward POC flux measurements were obtained at all sites from a free-drifting surface-tethered array (0-500 m) to which sediment traps were attached to measure the gravitational flux (Petiteau et al., *submitted*)[1]. Three sediment traps, located between 179 and 284 m depth, were deployed on the array for three days at each site. Three deployments were performed at SOTS while two deployments were performed at P1 (56 ° S) and P2 (58 ° S). Average POC flux (mmol m^2 d^{-1}) per trap was converted to mg C m^{-2} d^{-1} for direct comparison to the active flux estimated in the present study. To avoid misattribution of the pump fluxes, termed

1 Petiteau, L., Boyd, P. W., Le Moigne, F. A. C., Villa-Alfageme, M., Vioque, I., Laurenceau-Cornecé, E. C., et al. Microbial remineralization is a depth-varying contributor to particle flux attenuation in the Southern Ocean. *Global Biogeochemical Cycles. (Submitted)*.

double accounting, only the sediment traps deployed at the base of the epipelagic layer (SOTS: 179 - 185 m, P1: 189 m, and P2: 191 - 192 m depth) were used to compare with the active flux out of the epipelagic layer, defined arbitrarily as 200 m depth in this study.

2.5 Active acoustics

Acoustic data were collected using Simrad EK80 echosounders operating at two frequencies, 18 kHz and 38 kHz. These acoustic data, represented as echograms underwent processing in Echoview V.11.1.49 software, following IMOS open ocean standards and were analyzed qualitatively. Daytime and nighttime periods were simplified to 10:00 – 14:00 hours and 00:00 – 03:00 hours. Detailed methods are provided in the Supplementary material.

3 Results

3.1 Mesozooplankton abundance and community composition

Mesozooplankton abundance (ind. m^{-3}) was consistently higher at the two polar sites compared to SOTS. At SOTS, mesozooplankton abundance showed little variation between day and night, while at the polar sites, it increased by 81% at P1 and 68% at P2 during the night (Figure 2).

At all three sites, the mesozooplankton community was predominantly composed of copepods, accounting for an average of 90% at SOTS, 97% at P1, and 93% at P2 (Figure 2). At SOTS, the calanoid, *Neocalanus tonsus* made up an average (day & night) of 34% of the mesozooplankton community, while the cyclopoid, *Oithona* spp. contributed 17%, with the remainder consisting of other copepods and mesozooplankton. Farther south, the mesozooplankton abundance reflected a different community. At P1, the large calanoid, *Rhincalanus gigas* and *Oithona* spp. were the dominant taxa, contributing 32% and 21% of the mesozooplankton

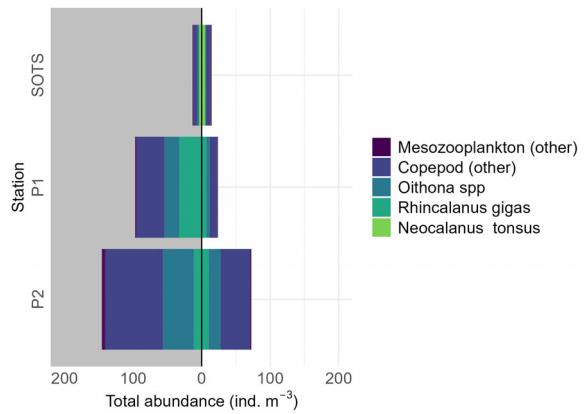

FIGURE 2
Mesozooplankton abundance (m^{-3}) per site, taxon, time of day (night = dark grey, day = white). Only one day and one night tow in the epipelagic layer (0 – 200 m) was conducted per site.

abundance, respectively. However, at P2, the abundance of *R. gigas* declined to an average of 7%, resulting in a community dominated by a more diverse assemblage of copepod taxa (Figure 2).

3.2 Micronekton biomass and community composition

Micronekton biomass followed a similar pattern to mesozooplankton abundance with higher biomass at the two polar sites compared to SOTS (Table 2). Like mesozooplankton abundance at SOTS, there was little variation in micronekton biomass between day and night, whereas biomass increased substantially at night at both polar sites.

Vertically resolved micronekton biomass revealed distinct patterns. At SOTS and P1, up to 80% of total water column (0 – 1000 m) micronekton biomass was concentrated in the epipelagic layer at night. During the day, biomass shifted, with up to 64% found in the upper mesopelagic layer (200 – 400 m). Pelagic tunicates dominated micronekton biomass across sites: *Pyrosoma atlanticum* at SOTS and *Salpa thompsoni* at P1 and P2. Fish were the dominant group in the lower mesopelagic layer across all three sites, accounting for up to 38% of biomass during the day and 65% of biomass at night (Figure 3). Krill contributed 17% of the nighttime epipelagic biomass at P2. See Supplementary Table 4 for percentage contribution and mg C m^{-3} of micronekton taxa per depth, site, and time of day and Supplementary Figures 1-5 for micronekton family-specific contributions to higher taxa biomass.

3.3 Active carbon export

Average active carbon export at 200 m depth by micronekton was highest at the polar sites compared to SOTS (Table 3). The average subsampled length of pyrosomes from this study (300 mm) resulted in a 2-3 order of magnitude increase in their CIP (21.4 mg C ind^{-1} d^{-1}) compared to most other taxa (0.18 – 2.29 mg C ind^{-1} d^{-1}, Table 4) (based on 12h at depth for site comparison). Fish also had comparatively high CIP (2.29 mg C ind^{-1} d^{-1} Table 4) (Figure 4).

At SOTS, fish, dominated by family Myctophidae contributed 54% (2.5 mg C m^{-2} d^{-1}) of micronekton MMP export (Figure 4). Despite the relatively low abundance at SOTS, pyrosomes made a disproportionately large contribution to downward carbon export, accounting for 23% (1.05 mg C m^{-2} d^{-1}) of the total micronekton export due to their large size and high average CIP. At P1,

TABLE 2 Micronekton mean total water column (0 – 1000 m) biomass (mg C m^{-3} ± SD) per site and time of day (Day/Night).

Site	Micro Day (mg C m^{-3} ± SD)	Micro Night (mg C m^{-3} ± SD)
SOTS	4.2 ± 2.5	3.6 ± 2.8
P1	4.8 ± 0.9	8.1 ± 5.5
P2	7.6 ± 1.2	4.9 ± 2.4

10.3389/fmars.2025.1461723

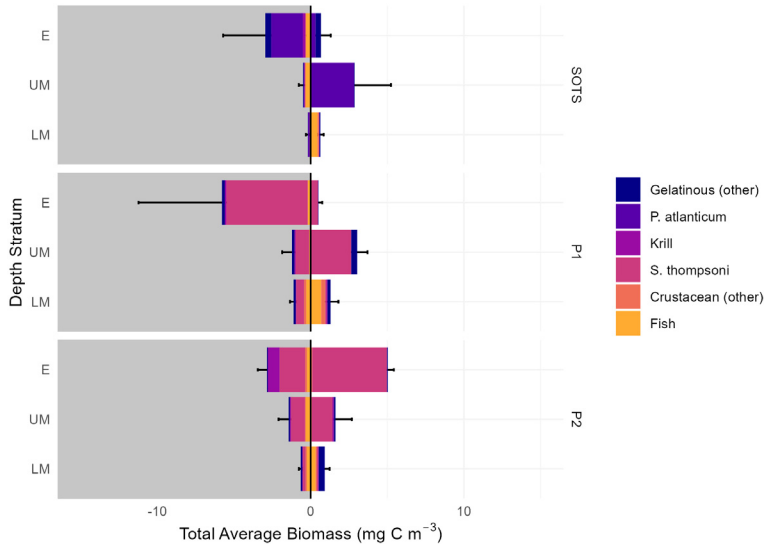

FIGURE 3
Average micronekton biomass (mg C m^{-3} ± SD) per site, taxon, time of day (night = dark grey, day = light grey) and depth stratum. E: epipelagic (0-200 m depth), UM: upper mesopelagic (200-400 m), LM: lower mesopelagic (400-1000 m).

micronekton export was dominated by *S. thompsoni*, contributing 7.7 mg C m^{-2} d^{-1} (83% of export), followed by fish contributing 1.1 mg C m^{-2} d^{-1}. At P2, export was split between krill contributing 2.7 mg C m^{-2} d^{-1} (34%), *S. thompsoni* contributing 2.5 mg C m^{-2} d^{-1} (32%) and fish 2.2 mg C m^{-2} d^{-1} (28%) with other gelatinous taxa making up the remaining 6% of the total micronekton carbon export (Figure 4).

Active carbon export by copepods was notably higher at the polar sites compared to SOTS. While the carbon injection potential (CIP) of *N. tonsus* and *R. gigas* was comparable (Table 4), *Oithona* spp. exhibited a CIP an order of magnitude lower due to their smaller average size (0.75 mm). The average size of *R. gigas* varied between the two polar sites, with individuals at P2 being 1.07 mm larger on average, leading to an increase of 0.001 mg C d^{-1} in CIP (Table 4). At SOTS, *N. tonsus* dominated, accounting for 93% of the copepod carbon export (Figure 4).

3.4 Passive vs. active carbon transport

MMP export (mg C m^{-2} d^{-1}) below 200 m depth was compared to POC flux measured by sediment traps deployed shallower than 200 m at each site (Figure 5). Micronekton contribution to MMP export was equivalent to ~3-6% of the mean carbon export driven by the BGP at SOTS, 2-14% at P1, and 8-12% at P2 (Table 5). Copepod contribution to MMP export was equivalent to 1% of the mean carbon export driven by the BGP at SOTS and 29% at P1, while at P2 the copepod contribution was equivalent to 26% of BGP. Total estimated MMP export was equivalent to 5% of the gravitational flux at SOTS and between 37and 35% at P1 and P2 (Figure 5). Mean gravitational flux measurements were the lowest at

TABLE 3 Total active carbon export at 200 m (mg C m^{-2} d^{-1}) by the micronekton and copepod communities.

Site	Micronekton (mg C m^{-2} d^{-1})	Copepod (mg C m^{-2} d^{-1})
SOTS	4.95 ± 1.47	0.74
P1	9.37 ± 6.29	32.2
P2	7.96 ± 1.58	20.3

TABLE 4 Carbon Injection Potential (CIP, ind^{-1} mg C d^{-1}) of average length per taxon observed.

Taxon	Average Length (mm)	Dry Weight (mg)	CIP (ind^{-1} mg C d^{-1})
Crustacean (other)	24	29.57	0.18
Fish	50	284.28	2.29
Gelatinous (other)	42	48.33	0.26
Krill	26	21.90	0.22
Pyrosome (*P. atlanticum*)	300	13611.36	21.40
Salp (*S. thompsoni*)	74	32.82	0.28
Copepod (*N. tonsus*)	1.9	0.26	0.003
Copepod (*R. gigas* – P1)	2.66	0.18	0.002
Copepod (*R. gigas* – P2)	3.73	0.28	0.003
Copepod (*Oithona* spp.)	0.75	0.0094	0.0003

Note that estimates are standardized to 12 h for comparison.

10.3389/fmars.2025.1461723

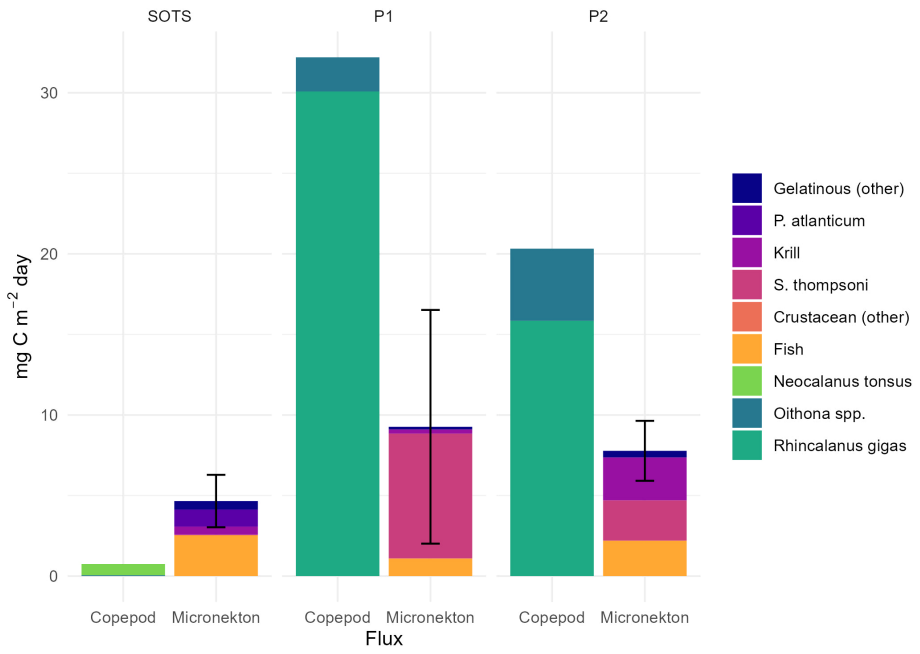

FIGURE 4
Active carbon export at 200 m depth per micronekton and copepod taxon and site (mg C m^{-2} d^{-1} +/- SD). Note, no SD provided for copepod contribution due to the lack of replicate tows.

the southernmost site (P2). See Supplementary Table 5 for flux comparison in mg C m^{-2} d^{-1}.

3.5 Active acoustics

Shipboard acoustic data collected on three representative days of site occupation (December 9th at SOTS, December 25th at P1, and January 5th at P2) revealed distinct backscatter patterns across the sites (Figure 6). At SOTS, high-intensity backscatter (reds and oranges) was consistently observed within the upper 200 m (Figure 6A) using the 18 kHz echosounder, persisting throughout the day and night. Additionally, a deep scattering layer between 500–800 m (Figure 6C) was detected with the 38 kHz echosounder, also present continuously over the diurnal cycle. Both echosounders revealed a region of low backscatter between 200–350 m during the day (Figure 6B).

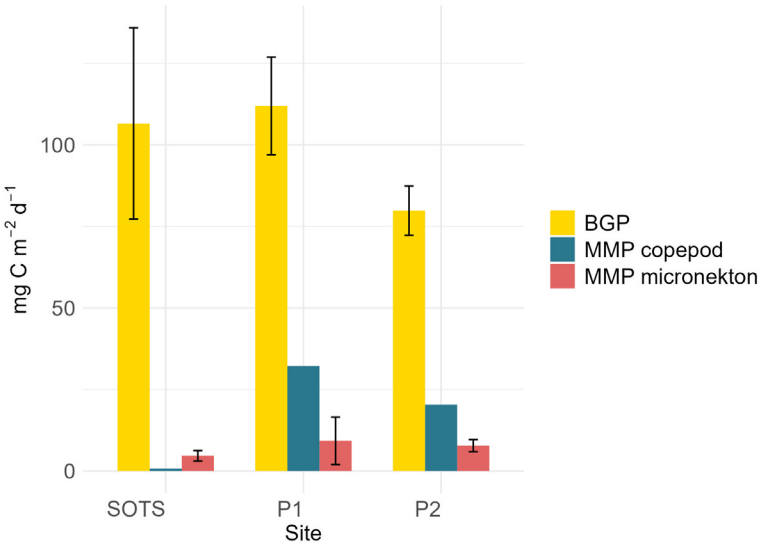

FIGURE 5
BGP v. MMP at 200 m (mg C m^{-2} d^{-1}). MMP includes micronekton (red) and copepod (blue) contribution. BGP was measured from sediment traps deployed ~10-20 m shallower than the 200 m depth horizon used for the MMP flux estimation.

10.3389/fmars.2025.1461723

TABLE 5 Mean (± SD) downward carbon export through the BGP vs. MMP at sample sites (mg C m^{-2} d^{-1}) and micronekton/copepod contribution in comparison to BGP (% BGP).

Site	BGP (mg C m^{-2} d^{-1})	MMP (mg C m^{-2} d^{-1})	% BGP (micro)	% BGP (meso)
SOTS	106.53 (± 29.33)	5.74 (± 1.47)	3-6	1
P1	111.93 (± 14.95)	41.24 (± 6.29)	2-14	29
P2	79.81 (± 7.56)	28.19 (± 1.63)	8-12	26

At the polar sites, backscatter signals were weaker compared to SOTS, with the lowest signal levels observed in the upper 600 m at P2, indicated by white pixels. Scattering layers were evident at depths of 400–600 m and 700–1000 m at both polar sites, with portions of these layers migrating to shallower depths at night (Figure 6D). Additionally, a weak scattering layer, represented by blues and greys, was identified at approximately 170 m at P2 (Figure 6E).

4 Discussion

The mesopelagic-migrant pump (MMP) is one of the least model-constrained particle injection pumps facilitating the export of carbon from the upper ocean to depth, due, in part, to a lack of *in-situ* observations. This research presents a summertime case study of the MMP at three Southern Ocean sites by (1) estimating the magnitude of MMP-driven downward carbon export below 200 m depth based on mesozooplankton/micronekton community composition and DVM, and (2) comparing MMP export estimates with those from the biological gravitational pump (BGP). Our results suggest an increase in the relative importance of the MMP compared to the BGP during summer south of the Polar Front, with MMP export at the polar sites between 35-37% relative to the gravitational flux at 200 m depth.

The term CIP is new to this study, but it allows us to better describe an abstract concept. By using this concept, we can assess the total contribution of an individual based on their size and taxon, providing a more nuanced understanding of how different species contribute to carbon export.

4.1 MMP driven downward carbon export

4.1.1 Mesozooplankton contribution to the MMP

The contribution of mesozooplankton, represented by the copepod community, to downward carbon export varied

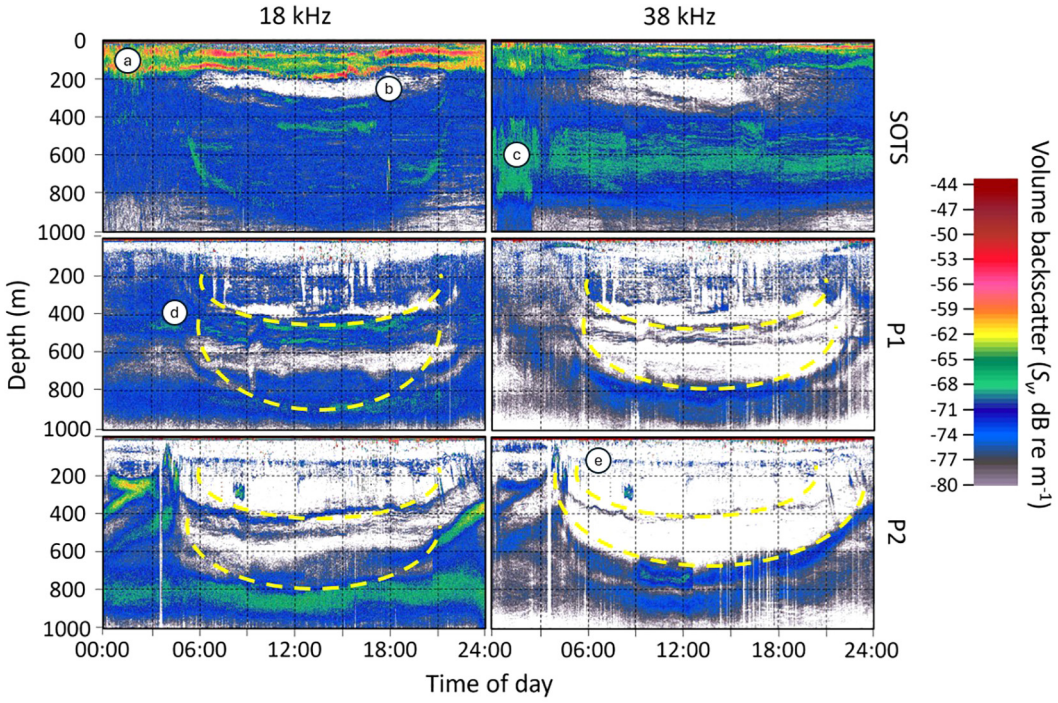

FIGURE 6
Echograms reflecting shipboard acoustics from three representative days during site occupation (December 9th at SOTS, Dec 25th at P1, Jan 5th at P2). **(A)** shows a high backscatter (reds and oranges) in the top 200; **(B)** shows a region of low backscatter regions (white pixels); **(C)** shows a deep scattering layer (blues and greens) between 500 – 800 m; **(D)** shows migration of biota from the deep scattering layer migration to surface; **(E)** shows a weak (i.e., denoted by blues and greys) non-migrating scattering layer at around 170 m. Yellow dashed lines represent migrating sound scattering layers.

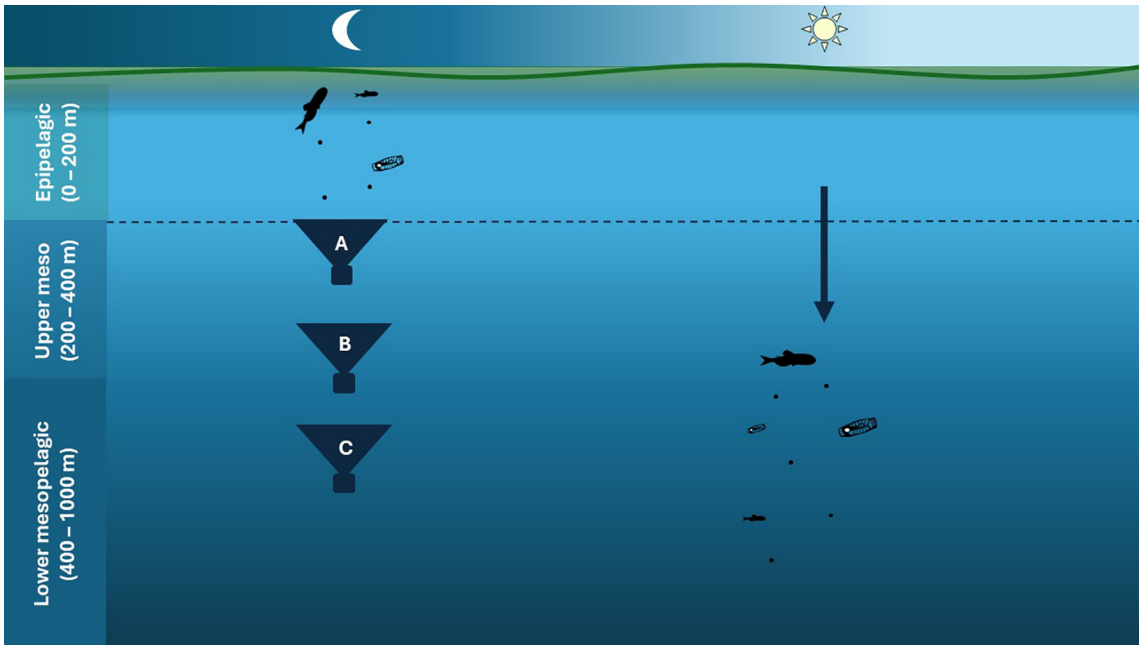

FIGURE 7
Schematic contrasting Dual Contribution vs. Double Accounting of POC in the BGP vs. MMP.**(A)** POC flux intercepted by a sediment trap at the base of the epipelagic zone (i.e. <200 m depth) includes fecal pellets from vertical migrators feeding at the surface at night. This POC, exported through the BGP, can be compared to POC injected below 200 m depth by migrators via the MMP (denoted by blue downwards arrow on right of the Figure). Thus, migrators contribute to both the BGP and MMP at ~200 m depth. **(B, C)** Are sediment traps deeper than 200 m depth. The POC flux intercepted by these traps may have been injected by migrators (i.e., potential double accounting). Since we could not determine the exact injection depth of the MMP from bioacoustics (Figure 5), this POC flux could represent either a dual contribution (if the injection depth is > depth of traps B and/or C) or double accounting (if injection depth is shallower than traps B and/or C).

substantially between the subantarctic and polar sites in this study. At the polar sites, mesozooplankton abundance was up to eight times higher than at SOTS, reflecting the typical distribution pattern of greater abundance and biomass in the Polar Frontal Zone, which decreases toward the north and south (Atkinson et al., 2012). However, diel vertical migration (DVM) behavior within the copepod community at each site both supports and diverges from previously reported trends, highlighting its complexity.

At SOTS, the persistence of the copepod population in surface waters throughout the day and night suggests both a high contribution to the recycling of carbon within the epipelagic zone and to the BGP by producing fecal pellets and carcasses instead of active carbon injection. The lack of DVM in *Neocalanus tonsus* during summer may align with its known ontogenetic migration pattern, which includes overwinter dormancy in the mesopelagic zone (Bradford-Grieve et al., 2001). While Cisewski et al. (2010) hypothesized that ontogenetic migrators may remain at the surface during summer to restore energy reserves depleted during their winter residence at depth, supporting our findings, additional observational data are needed to confirm whether a portion of the *N. tonsus* population participates in DVM during summer.

In contrast, our findings suggest increased migration by the copepod community at the polar sites, contributing to enhanced carbon export. At P1, despite lower overall copepod abundance compared to P2, export was higher due to a greater proportion of *Rhincalanus gigas* migrating. This is consistent with prior Southern Ocean studies reporting weak DVM in *R. gigas* during summer (e.g., Western Antarctic Peninsula; Conroy et al., 2020). However, other studies have observed ontogenetic migration in younger *R. gigas* copepodite stages (dominated by stage CIII) with a largely non-migratory late stage copepodite/adult community during summer (e.g., Scotia Sea; Atkinson, 1991) and little evidence of synchronized DVM during spring (Cook et al., 2023).

At P2, the higher relative proportion of *Oithona* spp., a species with lower CIP, resulted in reduced export compared to P1. However, *R. gigas* contributed 78% of the total export at P2 despite representing a smaller fraction of the migratory community, due to its order of magnitude higher CIP. These findings underscore the limitations of relying on representative species to estimate export, as size plays a critical role in CIP. While this study included *Oithona* spp. and *R. gigas*, representing the lower and upper size bounds captured by the Neuston net, it likely underestimates total export due to net biases, particularly of smaller species that pass through the mesh and the exclusion of the broader mesozooplankton community. Finally, the absence of replicate trawls limits the generalizability of these results, as observed abundance differences are based on single day and night sampling events. As such, we exercise caution in interpreting these findings.

4.1.2 Micronekton contribution to the MMP

Downward carbon export by micronekton was consistent across all sites, with estimates ranging from 5.0 to 9.4 mg C $m^{-2}d^{-1}$, despite differences in micronekton community composition and DVM behavior. Myctophids were dominant contributors to the MMP,

at SOTS, accounting for 54% of the micronekton-mediated export due to their high CIP. This finding aligns with previous research from the Southern Ocean south of Tasmania, where myctophids were similarly reported as major contributors to downward carbon export, with estimates ranging from 3.1 to 11.1 mg C $m^{-2}d^{-1}$ (Williams and Koslow, 1997). Globally, mesopelagic fish contribute around 16.1% (± 13%) to total carbon flux out of the euphotic zone (Saba et al., 2021).

While studies have traditionally focused on the role of fish in carbon export (Saba et al., 2021), there is increasing recognition of the potential contribution of gelatinous organisms. In this study, *Pyrosoma atlanticum* was the second most important taxon at SOTS, contributing 23% of the micronekton-mediated export despite its low abundance. A recent review (Lilly et al., 2023) reported *P. atlanticum* carbon flux estimates ranging from 10–15 mg C m^{-2} d^{-1} during periods of low stock (e.g., in the Tasman Sea during spring) to as high as 300–1000 mg C m^{-2} d^{-1} during large blooms in the southeast Atlantic Ocean (Drits et al., 1992). While the abundance of *P. atlanticum* observed in this study is at the lower end of this range, anecdotal observations from SOTS (RV *Investigator* voyage, personal communication, Halfter, 2019) suggest that larger blooms may occur into autumn. Similarly, *Salpa thompsoni* has been shown to induce significant export pulses in the Southern Ocean (Décima et al., 2023; Stone and Steinberg, 2016). A study conducted near the Chatham Rise (east of New Zealand) reported that salp blooms increased carbon export fivefold, with up to 46% of net primary production (NPP) transported to the mesopelagic zone (Décima et al., 2023). In this study, *S. thompsoni* contributed substantially to micronekton-mediated MMP export at the polar sites, accounting for 83% of export at P1 and 32% at P2.

However, uncertainties in allometric relationships can significantly affect CIP determination and overall export estimates. McMonagle et al. (2023) highlighted that fish-mediated carbon flux estimates can vary up to sixfold depending on the assumptions made in bioenergetic and movement models. Their analysis emphasized respiration as the most influential parameter affecting export estimates. Belcher et al. (2019) also identified that globally derived allometric equations for respiration often poorly represent colder regions. Given the paucity of Southern Ocean-specific data, some of the equations used in this study were globally derived (Supplementary Table 2). As a result, fish respiration at polar sites may have been underestimated by up to fourfold, although estimates at SOTS are likely more representative.

Biomass and abundance estimates for both micronekton and mesozooplankton in this study are also likely underestimated due to net selectivity and sampling biases. Smaller taxa, such as *Oithona* spp. and early developmental stages of krill, may pass through nets, leading to underrepresentation of their biomass (Irigoien et al., 2014). Conversely, larger, more mobile taxa like krill, cephalopods, and myctophids may evade capture due to their swimming abilities (Kwong et al., 2022). McMonagle et al. (2023) demonstrated that accounting for these sampling biases in sensitivity analyses can amplify export estimate ranges by at least tenfold. Furthermore, patchy distributions of taxa, such as krill swarms or salp chains, create uneven sampling challenges (Kwong et al., 2022). Although bootstrapping was employed in this study to mitigate these effects, it may not fully capture the inherent variability of micronekton and mesozooplankton distributions. In the absence of multinet sampling, which allows simultaneous sampling across the water column, bootstrapping provides an appropriate envelope of uncertainty.

4.1.3 Patterns in DVM

A notable difference in DVM behavior was observed in the salp population between P1 and P2, with more pronounced differences in day and night salp biomass within the upper 200 m at P1 compared to P2. This suggests suppressed salp DVM at P2 where site occupation coincided with peak chl-a concentrations (Boyd et al., 2024). Changes in DVM behavior, or adaptive DVM, have been observed previously in mesozooplankton and micronekton communities (Bandara et al., 2021; Hann et al., 2023). Reverse DVM (epipelagic layer during the day) as well as suppressed DVM (as observed in the salp community at P2 in this study) has implications for the magnitude of MMP export, thus, understanding the drivers of DVM is important in modeling efforts. In a study conducted off the Western Antarctic Peninsula, Hann et al. (2023) documented a pattern of suppressed *S. thompsoni* migration followed by weak DVM in late January, a trend analogous to the observations made at P2 and P1 in the present study. Significant positive correlations between salp abundances and chlorophyll-a biomass in the upper ocean (0 - 50 m), as observed by Hann et al. (2023), suggest that patterns in DVM behavior reflect changes in food availability. Applying this explanation to the present study, salps are likely exploiting phytoplankton in the upper ocean both day and night, as observed at P2 until significant depletion of upper ocean stocks takes place, upon which they initiate nocturnal DVM as observed at P1 when site occupation was past peak chl-a concentrations.

Despite the suppressed migration of salps, the export at P2 remained comparable to that of P1, largely owing to the presence of krill, specifically *Euphausia* spp., and myctophids. This trend contradicts the findings of Kwong et al. (2020), which suggested that variations in DVM led to significant differences in the magnitude of carbon export between cold and warm core eddies in the Tasman Sea. In the present study, we find other taxa playing a larger role in MMP export, compensating for decreases in export due to suppressed salp migration at P2. These findings underscore the complexities surrounding patterns of DVM and emphasize the importance of considering taxon-specific DVM behavior and associated linkages to environmental variables when assessing MMP-driven downward carbon export.

4.1.4 Injection depth

The RMT net used in this study lacked the vertical resolution required to precisely assess migration depth of the various taxonomic groups. Consequently, we were unable to confidently compare the MMP to the BGP below 200 m depth due to the risk of double counting POC as part of both processes.The depth at which carbon is respired or remineralized into DIC, referred to here as injection depth, is critical as it determines the duration of carbon

sequestration from the atmosphere (Nowicki et al., 2022). Studies employing multinets provide a significant advantage, offering community composition and biomass estimates throughout the water column and enabling quantitative assessments of injection depth and magnitude (Cook et al., 2023). Without a multinet, however, our injection depth analysis remains qualitative.

To supplement these limitations, ship-based acoustics from the SOLACE voyage provide a complementary method to infer migration depths of mesozooplankton and micronekton. By analyzing vertical and temporal differences in sound scattering layers (SSLs), acoustics reveal patterns that inform carbon injection depth (Annasawmy et al., 2019).

For this study, we used two acoustic frequencies: 18 kHz, which is selective towards small gas-bearing animals (e.g., larval fish or small fish), and 38 kHz, which is more sensitive to larger gas-bearing organisms (e.g., larger fish and siphonophores) and crustaceans. Migration patterns below 200 m were evident across all sites, with scattering layers observed at depths of 350–600 m (SOTS), 400–550 m (P1), and either 100–200 m or 350–450 m (P2). At SOTS, a strong 18 kHz signal suggests the presence of larval fish in the non-migrating surface layer and larger fish in deeper layers. The strong gas bladder signal from deeper layers, coupled with relatively low fish biomass estimates from net samples, likely reflects net avoidance by fish.

In contrast, weaker and patchy surface backscatter signals were observed at the polar sites. Given the prevalence of salps in these areas and their limited scattering ability at lower frequencies, gelatinous organisms are likely underrepresented in echograms. Higher acoustic frequencies, which can detect gelatinous taxa more effectively, attenuate more quickly at depth, complicating the determination of migration depths for these organisms.

Notable differences between day and night backscatter patterns in deep scattering layers across all sites indicate vertical migrations between upper and lower mesopelagic layers. These dynamics, though not included in this study's carbon export analysis, are likely significant. Predation by deep migrators (those descending from the lower to the upper mesopelagic) on shallow migrators (those rising from the upper mesopelagic to the epipelagic) could enhance carbon sequestration by rapidly transferring carbon to deeper layers upon returning to their daytime depths (Vinogradov, 1962). This highlights the importance of considering mesopelagic food web dynamics when assessing carbon storage in the water column in future studies (Nowicki et al., 2022).

4.2 The relative magnitudes of the MMP versus the BGP

A comparison of the MMP with the BGP at each sample site in this study allows us to: understand the relative importance of active carbon export in different environments and provide an estimate of how much export is overlooked if we only consider the BGP. However, despite a growing number of MMP observational studies, few report on this intercomparison due to a lack of concurrent BGP sampling. Of the published studies that have compared these two pumps (~ 200 m depth), the ratio observed in the current study falls within the reported range. For example, active export by the MMP was 18-43% relative to the BGP in the Western Equatorial Pacific during winter (Hidaka et al., 2001), 5-89% in the Canary Current during spring (Hernandez-Leon et al., 2019), 18-43% at the Bermuda Atlantic Time Series Site (BATS) during summer (Goldthwait and Steinberg, 2008) and 1.5-2.4% in the North Pacific Subtropical Gyre during summer (Pakhomov et al., 2019), noting that some of these studies focus on discrete aspects of the MMP (i.e., specific taxonomic groups or individual fluxes), making absolute comparisons across different studies challenging.

The MMP export at SOTS in the current study was 5-7 times lower than MMP export at the polar sites and equivalent to up to 5% relative to the BGP at 200 m depth. This difference in magnitude can be attributed to the tenfold higher biomass of migrating mesozooplankton at the polar sites when compared to SOTS. HNLC regions such as SOTS generally have higher carbon export efficiencies (ratio of export relative to primary production) than regions with higher productivity, due in part to the composition of primary consumers (Halfter et al., 2020). Reduced grazing pressure on phytoplankton stocks due to the low abundance of mesozooplankton relative to the polar sites leaves larger, ungrazed phytoplankton aggregates more readily exported by gravitational sinking (Steinberg and Landry, 2017). However, while the phytoplankton community at SOTS was dominated by large, fast sinking diatoms (Strzepek et al., *submitted*)[2], analysis of gel trap images taken from sediment traps deployed during SOLACE (Petiteau et al., *submitted*)[1] show gravitational export at the shallowest sediment trap was dominated by compact fecal aggregates and broken or intact fecal pellets ranging from 0.15-1.6 mm in length. Since pyrosomes and myctophids produce dense fecal pellets similar in size to particles found in the gel traps (Lilly et al, 2023; Saba and Steinberg, 2012), they may contribute to the BGP while feeding and egesting in the surface layers in addition to their active contribution to the MMP at depth. We term this a dual contribution, which is distinctly different from double accounting between PIPs (Figure 7).

Further south, the relative importance of the summertime MMP compared to the BGP increased, with export flux 37% and 35% equivalent to the BGP. Despite large differences in community composition and DVM behavior, MMP export at both polar sites was comparable. Therefore, at the polar sites, the relative importance of the MMP when compared to the BGP was contingent on the strength of the BGP. The smaller BGP export at P2 (peak seasonal chl-a in the upper ocean) when compared to P1 (after seasonal peak chl-a) may be attributed to a time lag between peak productivity and downward export below 200 m depth as reported by Savoye et al. (2008) in the Indian sector of the Southern Ocean (Kerguelen Plateau). In contrast to the SOTS site, gel traps at the polar sites were dominated by fluffy fecal aggregates, identified as reworked salp fecal pellets (Petiteau et al., *submitted*)[1]. This

2 Strzepek, R. F., Latour, P., Ellwood, M. J., Shaked, Y., and Boyd, P. W. Microbial competition for iron determines its availability to the Ferrous Wheel. *Proc. Natl. Acad. Sci. (Submitted)*.

suggests during a salp bloom, in addition to their active contribution through DVM, salps are also important passive exporters when feeding and egesting at the surface (Décima et al., 2023). However, the relative contribution of dominant taxa to different pumps across the sites may be contingent on the time of year.

4.2.1 Seasonality of the MMP in the Southern Ocean

The present study provides a summertime snapshot of the MMP. However, seasonal trends in zooplankton abundance, indicated by long-term acoustic backscatter monitoring, have been observed in the Southern Ocean (Cisewski et al., 2010; Cisewski and Strass, 2016; Trull et al., 2019). The relationship between the seasonality of zooplankton abundance and downward export may be complex. For example, Madin et al. (2001) reported weak correlations between total zooplankton biomass and export at the Bermuda Atlantic Time Series Site (BATS), and hence peak zooplankton abundance may not align with peak MMP export in the Southern Ocean. Trull et al. (2019) reported peak zooplankton abundance at SOTS in December (early summer), while Cisewski and Strass (2016) observed slightly later peaks (January-February; late summer) between 64-69°S in the eastern Weddell Sea. In both Southern Ocean regions peak mesozooplankton abundance coincided with peak primary productivity. These findings suggest that SOTS, and P2 (current study) were likely sampled during or just before periods of peak zooplankton abundance, whereas P1 was sampled slightly after the peak.

In the MMP, in addition to zooplankton abundance, their DVM behavior controls the magnitude of carbon injected at depth. Both Trull et al. (2019), Cisewski et al. (2010) and Cisewski and Strass, (2016) found minimal day-night differences in acoustic backscatter signals during periods of peak zooplankton abundances, indicating an absence of DVM. The absence of DVM during early summer in these studies suggests reduced MMP export at this time. Although the current study observed DVM based on RMT (micronekton) and neuston (mesozooplankton) net samples, the sound scattering layers present in the upper 200 m observed at all three sites suggest a non-migrating layer of the zooplankton community present at each site. This trend is especially conspicuous at SOTS with the higher intensity acoustics signal in the upper 200 m likely reflecting the presence of larval fish. According to Cisewski et al. (2010) and Trull et al. (2019), DVM initiates in late summer to early autumn, with zooplankton abundance tapering off into late autumn and reaching a seasonal low in winter in both the northern (SOTS) and southern regions (Weddell Sea). This decline in DVM likely reflects the ontogenetic migration of copepods, shifting carbon export from the MMP to the Seasonal Lipid Pump (SLP) (Bradford-Grieve et al., 2001). Therefore, MMP export is assumed to be highest in autumn, with a latitudinal lag between the SOTS and polar sites (Hunt and Hosie, 2006).

The initiation of DVM in autumn therefore may reflect the maturation of larvae, depletion of phytoplankton stocks and/or the enhanced advantage of DVM with increased darkness (Cisewski et al., 2010). At SOTS (this study) the non-migrating surface scattering layer was likely due to larval fish that are expected to mature and commence DVM by autumn (Williams and Koslow, 1997), enhancing the MMP. However, other important zooplankton exporters may not follow this trend. For instance, studies have shown that *S. thompsoni* can be found year-round (Atkinson et al., 2012), while others have observed that they overwinter at depth, a period during which they do not engage in DVM (Müller et al., 2022). Even less is known about the initiation of pyrosome blooms (Lilly et al, 2023). Given that gelatinous blooms can significantly enhance export (Décima et al., 2023), a better understanding of their life history and bloom initiation is crucial.

Interannual variation in zooplankton stocks can result in slightly different peak timings in abundance. Hunt and Hosie (2006) found peak abundances along the 140°E transect south of Tasmania to be February in the SAZ and March in the PFZ. To gain a more accurate indication of peak MMP export, it is essential to understand the timing of taxon-specific DVM initiation after peak abundance (summer-early autumn) and the timing of ontogenetic migration (late autumn-early winter) across various zooplankton taxonomic groups. Ultimately, understanding the strength and interaction of different PIPs throughout the year will enable better predictions of total downward carbon export in the Southern Ocean.

5 Conclusions

This study has provided examples of how an individual particle injection pump is operating at three distinct sites exposed to different environmental conditions in the Southern Ocean in summer, information that can be used to constrain carbon export models. Results from this study show that the MMP can be an important contributor to the BCP, and, by failing to consider trophic levels higher than primary production and mesozooplankton in Southern Ocean carbon export models, we may be missing a significant source of carbon exported out of the epipelagic zone. Results highlight the importance of considering community composition and DVM behavior. However, while assessing export across a depth horizon (200 m in this study) is a useful first step, it is important to consider the depth at which carbon is injected to understand sequestration time and to avoid the double accounting of POC across different pumps. Sound scattering layers from shipboard acoustics reveal the depth of migration from the surface ocean as well as more complex migrations at depth, a phenomenon not fully considered in this study. As migrations of predators within the mesopelagic can enhance the injection depth, additional analysis of food web interactions such as stable isotope analysis and ecological modeling are important next steps in modeling the biogeochemical fluxes driven by the MMP.

Our study has indicated that timescales are likely key considerations when comparing the different PIPs. Furthermore, there is evidence that the dominant taxonomic groups of vertical migrators contribute to export passively (BGP, when residing in the epipelagic) as well as actively (MMP, when residing in the mesopelagic). Importantly, this dual contribution differs from

double accounting since the location of the migrators in the water column will set their contribution to each pump, along with how each flux is measured.Their relative contribution to both pumps may change depending on environmental factors (like the stage of development of a phytoplankton bloom) and season. Accounting for taxon-specific thresholds in relative pump contribution and their importance in export flux would improve predictions of region-specific carbon export in the Southern Ocean, especially considering future climate change and exploitation scenarios. However, to accurately model the MMP, several limitations need to be addressed, including how to account for bias in sample methodology, better depth-resolved sampling, and the development of a representative sampling regime, capturing patchiness in abundance. Furthermore, this study highlights the current challenges and the opportunities for future MMP research.

Data availability statement

The raw data supporting the conclusions of this article will be made available by the authors, without undue reservation.

Ethics statement

The animal study was approved by Commonwealth Scientific and Industrial Research Organisation. The study was conducted in accordance with the local legislation and institutional requirements.

Author contributions

KB: Conceptualization, Formal analysis, Methodology, Writing – original draft, Writing – review & editing. SH: Conceptualization, Methodology, Supervision, Validation, Writing – review & editing. BS: Conceptualization, Data curation, Supervision, Writing – review & editing. KS: Writing – review & editing, Supervision. SR: Writing – review & editing, Formal analysis, Methodology. MB: Data curation, Writing – review & editing. CS: Writing – review & editing, Data curation. PB: Conceptualization, Supervision, Writing – review & editing.

Funding

The author(s) declare financial support was received for the research, authorship, and/or publication of this article. This work was funded by a PhD scholarship with the Australian Antarctic Program Partnership (AAPP) and by the Australian Research Council under the Laureate awarded to PB (FL160100131).

Acknowledgments

We acknowledge the use of the CSIRO Marine National Facility (https://ror.org/01mae9353) and grant of sea time on RV *Investigator* in undertaking this research. We thank the captain and crew of the RV Investigator as well as the efforts of the full SOLACE team. We extend particular thanks to Bree Woods, David Green, Annabelle Erskine, Inessa Corney and Margot Hind for their tireless efforts processing micronekton samples at sea.

Conflict of interest

The authors declare that the research was conducted in the absence of any commercial or financial relationships that could be construed as a potential conflict of interest.

Publisher's note

Supplementary material

The Supplementary Material for this article can be found online at: https://www.frontiersin.org/articles/10.3389/fmars.2025.1461723/full#supplementary-material

References

Al-Mutairi, H., and Landry, M. R. (2001). Active export of carbon and nitrogen at Station ALOHA by diel migrant zooplankton. *Deep-Sea Res. II* 48, 2083–2103. doi: 10.1016/S0967-0645(00)00174-0

Anderson, T. R., Martin, A. P., Lampitt, R. S., Trueman, C. N., Henson, S. A., and Mayor, D. J. (2019). Quantifying carbon fluxes from primary production to mesopelagic fish using a simple food web model. *ICES J. Mar. Sci.* 76, 690–701. doi: 10.1093/icesjms/fsx234

Annasawmy, P., Ternon, J. F., Cotel, P., Cherel, Y., Romanov, E. V., Roudaut, G., et al. (2019). Micronekton distributions and assemblages at two shallow seamounts of the south-western Indian Ocean: Insights from acoustics and mesopelagic trawl data. *Prog. Oceanography* 178, 1-21. doi: 10.1016/j.pocean.2019.102161

Archibald, K. M., Siegel, D. A., and Doney, S. C. (2019). Modeling the impact of zooplankton diel vertical migration on the carbon export flux of the biological pump. *Global Biogeochemical Cycles* 33, 181–199. doi: 10.1029/2018GB005983

Ariza, A., Garijo, J. C., Landeira, J. M., Bordes, F., and Hernandez-Leon, S. (2015). Migrant biomass and respiratory carbon flux by zooplankton and micronekton in the subtropical northeast Atlantic Ocean (Canary Islands). *Prog. Oceanography* 134, 330–342. doi: 10.1016/j.pocean.2015.03.003

Atkinson, A. (1991). Life cycles of *Calanoides acutus, Calanus simillimus and Rhincalanus gigas* (Copepoda: Calanoida) within the Scotia Sea. *Mar. Biol.* 109, 79–91. doi: 10.1007/BF01320234

Atkinson, A., Ward, P., Hunt, B. P. V., Pakhomov, E. A., and Hosie, G. W. (2012). An overview of Southern Ocean zooplankton data: Abundance, biomass, feeding and functional relationships. *CCAMLR Sci.* 19, 171–218.

Aumont, O., Maury, O., Lefort, S., and Bopp, L. (2018). Evaluating the potential impacts of the diurnal vertical migration by marine organisms on marine biogeochemistry. *Global Biogeochemical Cycles* 32, 1622–1643. doi: 10.1029/2018GB005886

Bandara, K., Varpe, Ø., Wijewardene, L., Tverberg, V., and Eiane, K. (2021). Two hundred years of zooplankton vertical migration research. *Biol. Rev.* 96, 1547–1589. doi: 10.1111/brv.12715

Belcher, A., Saunders, R. A., and Tarling, G. A. (2019). Respiration rates and active carbon flux of mesopelagic fishes (Family Myctophidae) in the Scotia Sea, Southern Ocean. *Mar. Ecol. Prog. Ser.* 610, 149–162. doi: 10.3354/meps12861

Bisson, K. M., Siegel, D. A., DeVries, T., Cael, B. B., and Buesseler, K. O. (2018). How data set characteristics influence ocean carbon export models. *Global Biogeochem. Cycles* 32, 1312–1328. doi: 10.1029/2018GB005934

Boyd, P. W., Antoine, D., Baldry, K., Cornec, M., Ellwood, M., Halfter, S., et al. (2024). Controls on polar Southern Ocean deep chlorophyll maxima: Viewpoints from multiple observational platforms. *Global Biogeochemical Cycles* 38, 1-21. doi: 10.1029/2023GB008033

Boyd, P. W., Claustre, H., Levy, M., Siegel, D. A., and Weber, T. (2019). Multi-faceted particle pumps drive carbon sequestration in the ocean. *Nature* 568, 327–335. doi: 10.1038/s41586-019-1098-2

Boyd, P. W., and Trull, T. W. (2007). Understanding the export of biogenic particles in oceanic waters: Is there consensus? *Prog. Oceanography* 72, 276–312. doi: 10.1016/j.pocean.2006.10.007

Bradford-Grieve, J. M., Nodder, S. D., Jillett, J. B., Currie, K., and Lassey, K. R. (2001). Potential contribution that the copepod *Neocalanus tonsus* makes to downward carbon flux in the Southern Ocean. *J. Plankton Res.* 23, 963–975. doi: 10.1093/plankt/23.9.963

Buesseler, K. O., and Boyd, P. W. (2009). Shedding light on processes that control particle export and flux attenuation in the twilight zone of the open ocean. *Limnology Oceanography* 54, 1210–1232. doi: 10.4319/lo.2009.54.4.1210

Burd, A. B., Hansell, D. A., Steinberg, D. K., Anderson, T. R., Arístegui, J., Baltar, F., et al. (2010). Assessing the apparent imbalance between geochemical and biochemical indicators of meso- and bathypelagic biological activity: What the @$! is wrong with present calculations of carbon budgets? *Deep-Sea Res. II* 57, 1557–1571. doi: 10.1016/j.dsr2.2010.02.022

Cisewski, B., and Strass, V. H. (2016). Acoustic insights into the zooplankton dynamics of the eastern Weddell Sea. *Prog. Oceanography* 144, 62–92. doi: 10.1016/j.pocean.2016.03.005

Cisewski, B., Strass, V. H., Rhein, M., and Krägefsky, S. (2010). Seasonal variation of diel vertical migration of zooplankton from ADCP backscatter time series data in the Lazarev Sea, Antarctica. *Deep-Sea Res. Part I: Oceanographic Res. Papers* 57, 78–94. doi: 10.1016/j.dsr.2009.10.005

Conroy, J. A., Steinberg, D. K., Thibodeau, P. S., and Schofield, O. (2020). Zooplankton diel vertical migration during Antarctic summer. *Deep-Sea Res. Part I: Oceanographic Res. Papers* 162, 1-15. doi: 10.1016/j.dsr.2020.103324

Cook, K. B., Belcher, A., Juez, D. B., Stowasser, G., Fielding, S., Saunders, R. A., et al. (2023). Carbon budgets of Scotia Sea mesopelagic zooplankton and micronekton communities during austral spring. *Deep-Sea Res. Part II: Topical Stud. Oceanography* 210, 1-15. doi: 10.1016/j.dsr2.2023.105296

Cotté, C., Ariza, A., Berne, A., Habasque, J., Lebourges-Dhaussy, A., Roudaut, G., et al. (2022). Macrozooplankton and micronekton diversity and associated carbon vertical patterns and fluxes under distinct productive conditions around the Kerguelen Islands. *J. Mar. Syst.* 226, 1-18. doi: 10.1016/j.jmarsys.2021.103650

Dall'Olmo, G., Dingle, J., Polimene, L., Brewin, R. J. W., and Claustre, H. (2016). Substantial energy input to the mesopelagic ecosystem from the seasonal mixed-layer pump. *Nat. Geosci.* 9, 820–823. doi: 10.1038/ngeo2818

Davison, P. C., Checkley, D. M., Koslow, J. A., and Barlow, J. (2013). Carbon export mediated by mesopelagic fishes in the northeast Pacific Ocean. *Prog. Oceanography* 116, 14–30. doi: 10.1016/j.pocean.2013.05.013

Décima, M., Stukel, M. R., Nodder, S. D., Gutiérrez-Rodríguez, A., Selph, K. E., dos Santos, A. L., et al. (2023). Salp blooms drive strong increases in passive carbon export in the Southern Ocean. *Nat. Commun.* 14, 425. doi: 10.1038/s41467-022-35204-6

Drits, A. V., Arashkevich, E. G., and Semenova, T. N. (1992). *Pyrosoma atlanticum* (Tunicata, Thaliacea): grazing impact on phytoplankton standing stock and role in organic carbon flux. *J. Plankton Res.* 14, 799–809. doi: 10.1093/plankt/14.6.799

Efron, B., and Tibshirani, R. (1993). *An introduction to the bootstrap.* (New York: Chapman and Hall).

Frenger, I., Landolfi, A., Kvale, K., Somes, C. J., Oschlies, A., Yao, W., et al. (2024). Misconceptions of the marine biological carbon pump in a changing climate: Thinking outside the "export" box. *Global Change Biol.* 30, 1-12. doi: 10.1111/gcb.17124

Goldblatt, R. H., Mackas, D. L., and Lewis, A. G. (1999). Mesozooplankton community characteristics in the NE subarctic Pacific. *Deep-Sea Res. II* 46, 2619–2644. doi: 10.1016/S0967-0645(99)00078-8

Goldthwait, S. A., and Steinberg, D. K. (2008). Elevated biomass of mesozooplankton and enhanced fecal pellet flux in cyclonic and mode-water eddies in the Sargasso Sea. *Deep-Sea Res. Part II: Topical Stud. Oceanography* 55, 1360–1377. doi: 10.1016/j.dsr2.2008.01.003

Halfter, S., Cavan, E. L., Butterworth, P., Swadling, K. M., and Boyd, P. W. (2021). Sinking dead"—How zooplankton carcasses contribute to particulate organic carbon flux in the subantarctic Southern Ocean. *Limnol. Oceonagraph.* 67, 13-25. doi: 10.1002/lno.11971

Halfter, S., Cavan, E. L., Swadling, K. M., Eriksen, R. S., and Boyd, P. W. (2020). The role of zooplankton in establishing carbon export regimes in the Southern Ocean – a comparison of two representative case studies in the subantarctic region. *Front. Mar. Sci.* , 7. doi: 10.3389/fmars.2020.567917

Halfter, S. (2019). *RV Investigator voyage, personal communication.*

Hann, A. M., Bernard, K. S., Kohut, J., Oliver, M. J., and Statscewich, H. (2023). New insight into *Salpa thompsoni* distribution via glider-borne acoustics. *Front. Mar. Sci.* 9. doi: 10.3389/fmars.2022.857560

Hernandez-Leon, S., Koppelmann, R., Fraile-Nuez, E., Bode, A., Mompeán, C., Irigoien, X., et al. (2020). Large deep-sea zooplankton biomass mirrors primary production in the global ocean. *Nat. Commun.* 11, 1–8. doi: 10.1038/s41467-020-19875-7

Hernandez-Leon, S., Putzeys, S., Almeida, C., Bécognée, P., Marrero-Díaz, A., Arístegui, J., et al. (2019). Carbon export through zooplankton active flux in the Canary Current. *J. Mar. Syst.* 189, 12–21. doi: 10.1016/j.jmarsys.2018.09.002

Hidaka, K., Kawaguchi, K., Murakami, M., and Takahashi, M. (2001). Downward transport of organic carbon by diel migratory micronekton in the western equatorial Pacific: its quantitative and qualitative importance. *Deep-Sea Res. I* 48, 1923–1939. doi: 10.1016/S0967-0637(01)00003-6

Hunt, B. P. V., and Hosie, G. W. (2006). The seasonal succession of zooplankton in the Southern Ocean south of Australia, part II: The Sub-Antarctic to Polar Frontal Zones. *Deep-Sea Res. Part I: Oceanographic Res. Papers* 53, 1203–1223. doi: 10.1016/j.dsr.2006.05.002

Irigoien, X., Klevjer, T. A., Røstad, A., Martinez, U., Boyra, G., Acuña, J. L., et al. (2014). Large mesopelagic fishes biomass and trophic efficiency in the open ocean. *Nat. Commun.* 5, 1–10. doi: 10.1038/ncomms4271

John, M. A. S., Borja, A., Chust, G., Heath, M., Grigorov, I., Mariani, P., et al. (2016). A dark hole in our understanding of marine ecosystems and their services: Perspectives from the mesopelagic community. *Front. Mar. Sci.* 3. doi: 10.3389/fmars.2016.00031

Jónasdóttir, S. H., Visser, A. W., Richardson, K., and Heath, M. R. (2015). Seasonal copepod lipid pump promotes carbon sequestration in the deep North Atlantic. *Proc. Natl. Acad. Sci. United States America* 112, 12122–12126. doi: 10.1073/pnas.1512110112

Kelly, T. B., Davison, P. C., Goericke, R., Landry, M. R., Ohman, M. D., and Stukel, M. R. (2019). The importance of mesozooplankton diel vertical migration for sustaining a mesopelagic food web. *Front. Mar. Sci.* 6. doi: 10.3389/fmars.2019.00508

Kwon, E. Y., Primeau, F., and Sarmiento, J. L. (2009). The impact of remineralization depth on the air-sea carbon balance. *Nat. Geosci.* 2, 630–635. doi: 10.1038/ngeo612

Kwong, L. E., Bahl, A. A., and Pakhomov, E. A. (2022). Variability in micronekton active carbon transport estimates on the Southwest Coast of Oahu using three different sampling gears. *Front. Mar. Sci.* 9. doi: 10.3389/fmars.2022.948485

Kwong, L. E., Henschke, N., Pakhomov, E. A., Everett, J. D., and Suthers, I. M. (2020). Mesozooplankton and micronekton active carbon transport in contrasting eddies. *Front. Mar. Sci.* 6. doi: 10.3389/fmars.2019.00825

Lilly, L. E., Suthers, I. M., Everett, J. D., and Richardson, A. J. (2023). A global review of pyrosomes: Shedding light on the ocean's elusive gelatinous "fire-bodies. *Limnol. Oceanography Lett.* 8, 812-829. doi: 10.1002/lol2.10350

Madin, L. P., Horgan, E. F., and Steinberg, D. K. (2001). Zooplankton at the Bermuda Atlantic Time-series Study (BATS) station: diel, seasonal and interannual variation in biomas- 1998. *Deep-Sea Res. II* 48, 2036–2082. doi: 10.1016/S0967-0645(00)00171-5

McMonagle, H., Llopiz, J. K., Hilborn, R., and Essington, T. E. (2023). High uncertainty in fish bioenergetics impedes precision of fish-mediated carbon transport estimates into the ocean's twilight zone. *Prog. Oceanography* 217, 1-19. doi: 10.1016/j.pocean.2023.103078

Mizdalski, E. (1988). *Weight and length data of zooplankton in the Weddell Sea in austral spring 1986* (Bremerhaven, Bundesrepublik Deutschland: Alfred-Wegener-Institut fur Polarforschung: Ber. Poiarforsch), 55.

Müller, S. J., Michael, K., Urso, I., Sales, G., De Pittà, C., Suberg, L., et al. (2022). Seasonal and form-specific gene expression signatures uncover different generational strategies of the pelagic tunicate during the southern ocean winter Salpa thompsoni. *Front. Mar. Sci.* 9, 1-15. doi: 10.3389/fmars.2022.914095

Nowicki, M., DeVries, T., and Siegel, D. A. (2022). Quantifying the carbon export and sequestration pathways of the ocean's biological carbon pump. *Global Biogeochemical Cycles* 36, 1–22. doi: 10.1029/2021GB007083

Nowicki, M., DeVries, T., and Siegel, D. A. (2024). The influence of air-sea CO2 disequilibrium on carbon sequestration by the ocean's biological pump. *Global Biogeochemical Cycles* 38, 1-17. doi: 10.1029/2023GB007880

Omand, M. M., D'asaro, E. A., Lee, C. M., Perry, M. J., Briggs, N., Cetinić, I., et al. (2015). Eddy-driven subduction exports particulate organic carbon from the spring bloom. *Science* 348, 222-225. doi: 10.1126/science.1260062

Pakhomov, E. A., Podeswa, Y., Hunt, B. P. V., and Kwong, L. E. (2019). Vertical distribution and active carbon transport by pelagic decapods in the North Pacific Subtropical Gyre. *ICES J. Mar. Sci.* 76, 702–717. doi: 10.1093/icesjms/fsy134

Phillips, B., Kremer, P., and Madin, L. P. (2009). Defecation by *Salpa thompsoni* and its contribution to vertical flux in the Southern Ocean. *Mar. Biol.* 156, 455–467. doi: 10.1007/s00227-008-1099-4

Saba, G. K., Burd, A. B., Dunne, J. P., Hernandez-Leon, S., Martin, A. H., Rose, K. A., et al. (2021). Toward a better understanding of fish-based contribution to ocean carbon flux. *Limnology Oceanography* 66, 1639–1664. doi: 10.1002/lno.11709

Saba, G. K., and Steinberg, D. K. (2012). Abundance, composition, and sinking rates of fish fecal pellets in the Santa Barbara channel. *Sci. Rep.* 2, 1–6. doi: 10.1038/srep00716

Savoye, N., Trull, T. W., Jacquet, S. H. M., Navez, J., and Dehairs, F. (2008). 234Th-based export fluxes during a natural iron fertilization experiment in the Southern Ocean (KEOPS). *Deep-Sea Res. II* 55, 841–855. doi: 10.1016/j.dsr2.2007.12.036

Smith, A. J. R., Wotherspoon, S. J., and Cox, M. J. (2023). Per-length biomass estimates of Antarctic krill (*Euphausia superba*). *Front. Mar. Sci*. 10. doi: 10.3389/fmars.2023.1107567

Steinberg, D. K., and Landry, M. R. (2017). Zooplankton and the ocean carbon cycle. *Annu. Rev. Mar. Sci.* 9, 413–444. doi: 10.1146/annurev-marine-010814-015924

Steinberg, D. K., Steinberg, D. K., Carlson, C. A., Bates, N. R., Goldthwait, S. A., Madin, L. P., et al. (2000). Zooplankton vertical migration and the active transport of dissolved organic and inorganic carbon in the Sargasso Sea. *Deep-Sea Res. I* 47, 137–158. doi: 10.1016/S0967-0637(99)00052-7

Stone, J. P., and Steinberg, D. K. (2016). Salp contributions to vertical carbon flux in the Sargasso Sea. *Deep-Sea Res. I* 113, 90–100. doi: 10.1016/j.dsr.2016.04.007

Thompson, A. F., Dove, L. A., Flint, E., Boyd, P. W., and Lacour, L. (2023). Interactions between multiple physical particle injection pumps in the Southern Ocean. *ESS Open Arch.* doi: 10.22541/essoar.168057558.87192564/v1

Trull, T. W., Bray, S. G., Manganini, S. J., Honjo, S., and François, R. (2001). Moored sediment trap measurements of carbon export in the Subantarctic and Polar Frontal Zones of the Southern Ocean, south of Australia. *J. Geophysical Res.* 106, 31489–31509. doi: 10.1029/2000jc000308

Trull, T. W., Jansen, P., Schulz, E., Weeding, B., Davies, D. M., and Bray, S. G. (2019). Autonomous multi-trophic observations of productivity and export at the Australian Southern Ocean time series (SOTS) reveal sequential mechanisms of physical-biological coupling. *Front. Mar. Sci.* 6. doi: 10.3389/fmars.2019.00525

Trull, T. W., Schulz, E., Bray, S. G., Pender, L., McLaughlan, D., Tilbrook, B., et al. (2010). The Australian integrated marine observing system southern ocean time series facility. *Oceans'10 IEEE Sydney*, 1-7. doi: 10.1109/OCEANSSYD.2010.5603514

Underwood, M. J., García-Seoane, E., Klevjer, T. A., Macaulay, G. J., and Melle, W. (2020). An acoustic method to observe the distribution and behaviour of mesopelagic organisms in front of a trawl. *Deep-Sea Res. Part II* 180, 1–7. doi: 10.1016/j.dsr2.2020.104873

Vinogradov, M. E. (1962). Feeding of deep-sea zooplankton. *Rapports Proces-Verbaux Des. Reunions* 153, 114–120.

Williams, A., and Koslow, J. A. (1997). Species composition, biomass and vertical distribution of micronekton over the mid-slope region off southern Tasmania, Australia. *Mar. Biol.* 130, 259–276. doi: 10.1007/s002270050246